Turbulence in high-beta ASDEX Upgrade advanced scenarios

H. Doerk,[1] A. Bock,[1] A. Di Siena,[1] E. Fable,[1] T. Görler,[1]
F. Jenko,[1] J. Stober,[1] and The ASDEX Upgrade Team[1]

[1] *Max-Planck-Institut für Plasmaphysik, Boltzmannstraße 2, D-85748 Garching, Germany*

Recent experiments at ASDEX Upgrade achieve non-inductive operation in full tungsten wall conditions by applying electron cyclotron and neutral beam current drive. These discharges are characterised by a well-measured safety factor profile, which does not drop below one, and a good energy confinement. By reproducing the experimental heat fluxes, nonlinear gyrokinetic simulations suggest that the observed strong peaking of the ion temperature in the core is caused by the stabilising impact of a significant beam ion content, as well as strong electromagnetic effects on turbulent transport. Quasilinear transport models are not yet applicable in this interesting and reactor relevant parameter regime, but available simulation data may serve as a testbed for improvements. As the present plasma is close to the kinetic ballooning (KBM) threshold, elevating the safety factor profile under otherwise identical conditions is proposed to clarify, whether profiles are ultimately limited by KBM turbulence, or by global stability constraints.

I. INTRODUCTION

Advanced tokamak studies have recently been successfully resumed at ASDEX Upgrade with a full tungsten wall [1–3]. With the overall goal of developing improved confinement regimes for steady state operation, the use of external current drive from neutral beam injection and electron cyclotron heating systems, as well as a high bootstrap current are essential. Here, we analyse a non-inductive scenario that is characterised by a safety factor $q > 1$ in the center, as well as good confinement with H_{98} around unity. In particular, the ion temperature becomes strongly peaked in the core during the final high-β phase ($\beta_N \sim 2.7$), while transport levels still remain well above the neoclassical level. Linear and nonlinear gyrokinetic simulation data is lacking thus far and this gap is closed in this paper. It is demonstrated that the reduction of ion temperature gradient driven (ITG) turbulence due to dilution by beam ions, as well as by nonlinear electromagnetic effects is key for accessing the steep ion temperature.

ITG turbulence stabilisation due to electromagnetic effects has been observed in many cases in the literature [4–6], and a correlation with increased relative strength of zonal flows is found [7, 8]. However, the opposite trend of increased transport at increased β has been documented in some strongly driven regimes as well. The relevance of fast ions for turbulent transport has been established experimentally in the course of developing improved H-modes or transport barriers (see e.g. Ref. [9]), and in gyrokinetic modelling [10]. Comprehensive nonlinear gyrokinetic results are available since half a decade, reaching from virtually electrostatic low density DIII-D QH modes [11], to strongly electromagnetic JET L-modes [12] and H-modes [8, 13, 14]. As shown in the course of this paper, the present ASDEX Upgrade non-inductive scenario is similar to the plasmas of the latter, strongly electromagnetic category. Core turbulence is close to a regime transition between ITG, which is reduced by electromagnetic effects and the presence of fast ions, on the one hand, and kinetic ballooning turbulence on the other hand. The latter is labelled as KBM/BAE regime, as it is driven by thermal and fast pressure gradients and features the characteristic frequency of the beta induced fast ion Alfvénic (BAE) modes. It is important to stress the necessity of including fast ions as a dynamic species in fully electromagnetic simulations for these plasmas. Analysing turbulent fast ion transport in the electrostatic limit or in the trace limit may be valid only in other plasma conditions [15].

For the present type of AUG discharges, H_{98} increases by about 15% due to electromagnetic and fast ion effects. Since this is due to a significant temperature peaking in the inner core, parameters like the fusion power are expected to increase even more strongly. Based on a gyrokinetic study for JET plasmas [8] a 20% improvement of the fusion power is estimated for an ITER hybrid reference case, highlighting the importance of gaining a detailed physics understanding. To this aim, a nonlinear gyrokinetic study is presented, which involves about 50 expensive nonlinear simulations, including flux-matching, parameter variations, and convergence tests. While such a study reveals the necessary physics ingredients for modelling advanced tokamak discharges, scenario development requires the use of fast (simplified) tools, such as quasilinear models. However, those models have to be extended in order to correctly describe and predict the improved confinement in the present regime.

For example, the trapped Gyro Landau Fluid code TGLF has been successfully used to describe plasma transport in the past [16–18], but for the present case, it overestimates the ion heat trans-

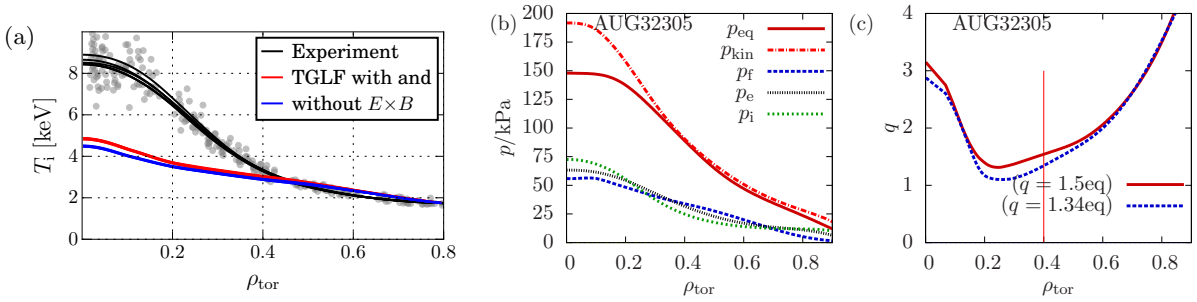

Figure 1: (a) AUG #32305 ion temperature profile measurements compared to ASTRA/TGLF modelling (reproduced from Ref. [3] (b) Pressure profiles q=1.34 eq., thermal species, fast particles. Summing the pressure of all species yields $p_{\rm kin}$, which is largely consistent with the equilibrium reconstruction $p_{\rm eq.}$. (c) q profiles q=1.34 eq. and q=1.54 eq., covering the error margin from IDE at $\rho_{\rm tor} = 0.4$.

port with both SAT0 and SAT1 saturation rules. As a result, the predicted ion temperature is much less peaked than the one measured in the experiment [1, 2]. In addition to the lack of nonlinear electromagnetic stabilisation physics, further limitations to quasilinear tools are known. While in the present ASDEX Upgrade scenario, impurity content and plasma rotation play a minor role for the turbulence regime, this is different under JET L-mode conditions: Including impurities and rotation in quasilinear models leads to more strongly peaked T_i than measured [19, 20]. For accurate extrapolation, both stabilising and destabilising trends need to be captured, which is subject of ongoing development. Besides improving the general understanding of transport physics in advanced tokamak scenarios, an important goal of this work is thus to provide well-resolved high realism nonlinear simulation data for developing and training simplified tools. This is an important step towards exploring promising operational spaces in future devices.

This paper is organised as follows. In Sec. II, we introduce the experimental conditions. In Sec. III the setup for gyrokinetic simulations is explained, and in Sec. IV the results are presented, performing a sensitivity analysis on the equilibrium reconstruction. Insights on the impact of fast ions on KBM and ITG physics is gained in Sec. V, and in Sec. VI linear and nonlinear GENE is compared to quasilinear TGLF simulations. Conclusions are drawn in Sec. VII.

II. EXPERIMENTAL PARAMETERS

We chose the AUG advanced tokamak discharge #32305 for our analysis, as this type of operation scenario promises steady-state tokamak operation and simultaneously good confinement quality [1–3, 21, 22]. The discharge is feedback controlled on β_N with two steady state phases obtained at $\beta_N =$ 2.0 and $\beta_N = 2.7$. In the high-β phase between 3.5 s and 4.0 s, a strongly peaked ion temperature profile is observed in the inner radii $\rho_{\rm tor} < 0.4$. The ion logarithmic temperature gradient $a/L_{Ti} = -a/T_i \partial_x T_i$ takes values about 2.7, which is twice as large as in the earlier low β_N phase.

In Ref. [3], the discharge evolution is followed with ASTRA/TGLF modelling [23, 24]. In previous investigations the plasma transport has been successfully modelled using TGLF [16, 17], for instance in a non-inductive H-mode scenario in DIII-D [25] or for H-modes with varying heating mixes in ASDEX Upgrade [26]. Also in the $\beta_N = 2.0$ phase of discharge 32305, ASTRA/TGLF predicts profiles, which are consistent with the experimental data. However, the strong ion temperature peaking at $\beta_N = 2.7$ is not reproduced. Despite the electron profile being captured relatively well, TGLF predicts $a/L_{Ti} \sim 0.8$, much lower than the experiment. This suggests nonlinear electromagnetic physics and fast ion effects to be responsible for the strong ion transport reduction as concluded in [12, 27] for a JET L-mode plasma, as well as JET H-mode plasmas [8, 13, 14]. For the gyrokinetic analysis, we focus on the radial position $\rho_{\rm tor} = 0.4$, where a/L_{Ti} becomes large and starts to deviate from TGLF predictions. Physical quantities are time-averaged between 3.5 s and 4 s for code input. The profiles of beam ion density and pressure are computed by TRANSP/NUBEAM [28, 29]. The magnetic equilibrium is reconstructed by the IDE approach integrating information from several q profile measurement techniques —motional stark effect (MSE), imaging MSE and Faraday angle diagnostics [30, 31]. As seen in Fig. 1(b), the pressure profile from the equilibrium reconstruction is largely consistent with the direct measurement. This leads to the remarkably small uncertainty of about ±10% of the q-profile, especially in the analysis region $\rho_{\rm tor} \approx 0.4$. For sensitivity analysis, we nevertheless generate two alternative time-averaged equilibria, their q-profiles being shown in

Fig. 1(c). At $\rho_{\rm tor} = 0.4$ the lower value is q=1.34 and the upper value is q=1.54, covering the uncertainty range of q around this radial position. The q-profile shown in Ref. [3] is taken at t=3.7 and has q=1.45 at $\rho_{\rm tor}$=0.4 and features a less prominent increase towards the axis. Besides the values of q and $\hat{s} = (x/q)\partial q/\partial x$, equilibrium changes affect the mapping from $\rho_{\rm tor}$ to the radial co-ordinate $x = r/a$. In our case, this results in up to 7% changes in the gradients a/L_T and a/L_n. Close to mode transitions, such small changes can be decisive, but it is shown in the following section that physics effects have a much stronger impact.

	q=1.34 eq.	q=1.54 eq.
$\nu_{ei}/(c_s/a)$	0.02	0.02
β_e[%]	1.426	1.411
q	1.542	1.343
$\hat{s}$	0.444	0.771
α_{tot}	0.711	1.00
α_{th}	0.504	0.614
$\gamma_{E\times B}/(c_s/a)$	0.06	0.058
$a[m]$	0.465	0.463
R/a	3.682	3.678
	$T_{0e} = 3.459\,\mathrm{keV}$	$n_{0e} = 5.73^{19}/\mathrm{m}^3$
from TRANSP:	$\langle Q_i V' \rangle = 2.488\,\mathrm{MW}$	$\langle Q_e V' \rangle = 1.961\,\mathrm{MW}$

Table I: $\rho_{\rm tor} = 0.4$ plasma parameters for two equilibrium reconstructions, $t = 3.5$ -4 s average.

	e	D	f
T_0/T_{0e}	1.000	0.982	7.899
n_0/n_{0e}	1.000	0.864	0.136
a/L_T	1.830	2.591	0.472
a/L_n	1.034	0.937	1.652

Table II: Electron (e), Deuterium (D) and beam ion (f) parameters for $\rho_{\rm tor} = 0.4$ q=1.34 eq., $t = 3.5$-4 s average.

III. SETUP FOR GYROKINETIC SIMULATIONS

We use the gyrokinetic code GENE in the flux-tube framework that involves Fourier representation in radial and in bi-normal (y) space [32, 33]. For ion-scale turbulence, the perpendicular domain $l_x = l_y = 128\rho_s$ is resolved with $n_x = 256$ and $n_y = 128$ grid cells, so that modes up to $k_y\rho_s \sim 3.5$ are taken into account. Here, $\rho_s = c_s/\Omega_i$ is the reference gyroradius, $c_s = (T_{0e}/m_D)^{0.5}$ is the reference (sound-) velocity and Ω_i is the ion Larmor frequency. Three species are included by default: electrons, thermal deuterium and beam deuterium ions. Due to low $Z_{\rm eff} \lesssim 1.2$, impurities can be safely neglected in these plasmas. To fully capture the electromagnetic (EM) response, perpendicular and parallel magnetic fluctuations are considered. Some runs are performed in the electrostatic (ES) limit of $\beta_e = 10^{-4}$, which is equivalent to neglecting $A_\parallel$ and $B_\parallel$ fluctuations. Employing the δf method, the distribution is split into a static Maxwellian background F_0 and a small, fluctuating part f_1. For beam ions, the equivalent temperature $T_f = p_f/n_f$ is assumed. Employing a recent development of GENE allowing arbitrary F_0 [34], we have verified that growth rates are rather robust with respect to exchanging the equivalent Maxwellian of the beam ions by an appropriate (yet isotropic) slowing down distribution. The impact of beam ions on turbulence can be threefold, as they (i) dilute the main ion species [9], (ii) increase geometric stabilisation [35], and (iii) dynamically contribute to plasma fluctuations (beyond dilution) [11, 36]. The latter can significantly reduce turbulence levels in nonlinear simulations [12, 27], but is also known to excite energetic particle modes and de-stabilise electromagnetic turbulence [8, 14]. The geometric effects of fast particles are mainly expressed by their contribution to the normalized pressure gradient $\alpha_{\rm geo} = -2q^2R/(\mu_0 B)(\nabla p/p)$, which is part of the magnetic equilibrium. This parameter should be consistent with $\alpha_{\rm kin} = q^2\beta_e \sum_j p_j/p_e(R/L_{nj}+R/L_{Tj})$ computed from the measured kinetic profiles. In our case, the equilibrium pressure from the Grad-Shafranov solver is only about 10% smaller than the measurement.

Fitting the coefficients of an analytical Miller-type geometry to the numerical equilibrium allows to set $\alpha_{\rm geo}$ and $\alpha_{\rm kin}$ independently. Keeping them consistent is considered most realistic, because it captures sensitive balance between stabilising and de-stabilising effects. Default Miller-type equilibria do not account for up-down asymmetry, but we have confirmed that the growth rates of ITG and KBM/BAE modes are in excellent agreement with the numerical equilibrium when $\alpha_{\rm geo}$ is matched. The pressure contribution to the magnetic drifts (see e.g. Ref. [37]) is kept self-consistent with $\alpha_{\rm geo}$ in this work.

In nonlinear simulations, the experimentally determined toroidal rotation profile is accounted for by means of including a parallel flow shear rate $\gamma_{\rm pfs}$, and an $E \times B$ shearing rate $\hat{\gamma}_E = (r/q)\,\mathrm{d}\Omega_{\rm tor}/\mathrm{d}r$ [38], which is modelled by k_y-dependent periodic shifts in k_x.

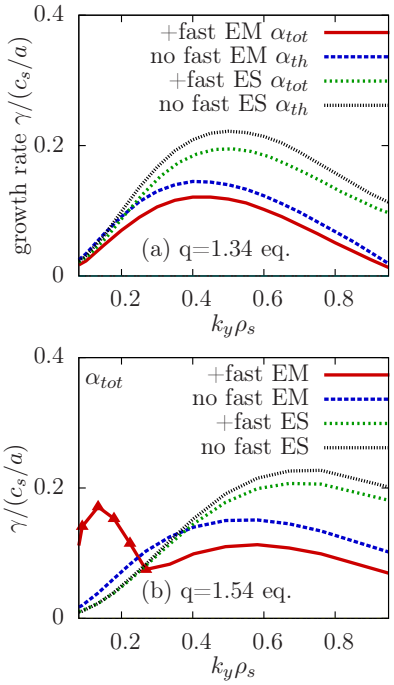

Figure 2: Linear growth rate spectra highlighting fast ion and EM effects in microinstabilities (a) for q=1.34 eq. and (b) for q=1.54 eq., the latter using $\alpha_{\rm geo} = \alpha_{\rm th} + \alpha_{\rm fast}$ even in the cases without fast ions.

IV. NONLINEAR GYROKINETIC SIMULATIONS

For the nominal parameters in Tables I,II we find ITG modes to be unstable for both q-profiles, as shown in Fig. 2, where EM and ES results with and without fast ions are shown. KBM/BAE modes occur at lower wavenumbers $k_y\rho_s < 0.2$ only in the $q = 1.54$ full physics case. The main difference of geometric parameters is found in q and $\hat{s}$. The complete GENE input files are found in the supplementary material of this paper.

Nonlinear simulations allow to match gyrokinetic predictions to experimental flux levels. This helps to identify the relevant physics behind the gradient up-shift between low-β and high-β phases. Scans in the main driving gradient a/L_{Ti} are useful to determine the sensitivity to this parameter, which is usually referred to as "stiffness". In Fig. 3 the flux-gradient relation is shown for (a) the q=1.34 and (b) the q=1.54 equilibria, and the heat flux level is compared to the TRANSP power balance result marked as "(exp)".

Even if large variations in a/L_{Ti} are performed, the experimental transport level can only be reconciled when the full EM response, as well as fast ions are included in the simulations. For comparison, ES simulations are performed, only neglecting magnetic fluctuations by setting $\beta = 10^{-4}$, while $\alpha_{\rm geo}$ is unchanged. The alternative of setting $\alpha_{\rm geo}$ small and consistent with β is confirmed to not significantly alter the result of vast over-prediction of transport in the ES case.

The results presented in Fig. 3 can be viewed as a sensitivity study in the equilibrium reconstruction, in particular in the q profile. In the ES limit, the heat flux is slightly larger at larger q. This is expected from the well-known $\hat{s}/q$ scaling of the critical gradient a/L_T that is related to the connection length qR [39]. It is important to mention that this a/L_T up-shift with $\hat{s}/q$ holds for electrostatic ITG with adiabatic electrons, which is not actually applicable to the strongly electromagnetic case: Linear electromagnetic stabilisation or substantial nonlinear critical gradient up-shifts become stronger with increased q. Furthermore, the full physics EM case with fast ions features a transition to KBM turbulence when increasing q from 1.34 to 1.54 at nominal gradients. Within the uncertainties, electron and ion thermal transport levels agree well with power balance results for both q profiles. In the $q = 1.54$ case, the fast ion gradients are flattened by 20%, while $\alpha_{\rm geo}$ includes full fast ion pressure (similar to the procedure in Ref. [8]), as otherwise the transition to KBM/BAE turbulence yields large transport levels.

Here, only ion-scale turbulence is included. Adding electron scale (ETG) turbulence and multiscale interaction may slightly increase the ratio Q_e/Q_i. Equilibrium $E \times B$ flow shear and the parallel velocity gradient (PVG) are always kept consistent with purely toroidal rotation. For specific JET plasmas, it has been documented that stiffness reduction due to increased $E \times B$ flow is partially compensated by the consistent increase of the PVG [40]. The same trends apply to the present ASDEX Upgrade scenario, but in a weakened fashion: Growth rates are barely affected by PVG and turbulence levels do not drop significantly due to $E \times B$ flow shear in fully electromagnetic simulations.

In order to isolate the effect of fast ions, electromagnetic simulations with only two species are performed. For the $q = 1.34$ equilibrium, two approaches for chosing the thermal ion density and density gradient are compared: The dilution limit eliminates the active fast ion species, leaving n_i and a/L_{ni}, as well as $\alpha_{\rm geo}$ unchanged. These simulations then violate quasineutrality. The dilution cases yield low fluxes close to the full physics case, showing the trend of reduced flux at higher gradient. The alternative is to preserve quasineutrality by setting $n_i = n_e$ and $a/L_{ni} = a/L_{ne}$, as done in Ref. [8], for example. Simulations of this second type prove to be very challenging, regardless if thermal $\alpha_{\rm th}$ or total pressure $\alpha_{\rm tot}$ is set in the geometry; The fluctuating amplitude increases

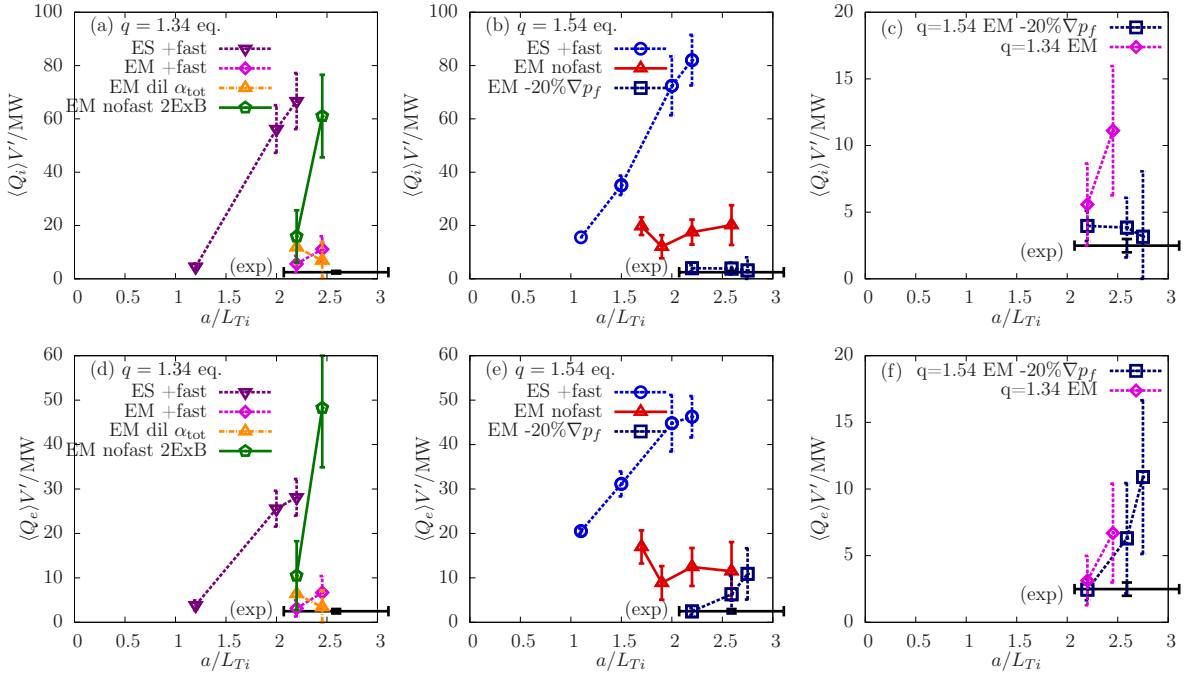

Figure 3: Flux-gradient relation from nonlinear GENE: (a) q=1.34 eq. includes fast ion pressure in α_{geo}. (b) for q=1.54 eq. includes full fast ion pressure in α_{geo}, but reduces the driving ∇p_f by 20% in the EM case. (c) zoom: matching the experiment with fast ions and EM effects. (d-f) electron flux Q_e.

with time and no statistically stationary state is reached. The simulations become stable when double values of the $E \times B$ rate and PVG are set. The data labelled as "no fast" in Fig. 3 is obtained in this way. Remarkably, both the electrostatic case, and the full physics case are not strongly sensitive to increasing $E \times B$ and PVG. The reason for this behavior remains unclear. These results, however, indicate that the reduction of main ion density and gradient is the main cause of turbulence stabilisation due to fast ions here.

Importantly, only in the full physics case can the experimental heat fluxes be reproduced by gyrokinetic simulations: neglecting electromagnetic effects or the dilution due to fast ions yield transport levels well above the experimental level. Thus, electromagnetic stabilisation and the presence of fast ions are key to accessing the steep ion temperature in high-β ASDEX Upgrade non-inductive plasmas. Consequences of the closeness to the KBM/BAE transitions are drawn in Sec. VII, after some of its properties are described in the following section.

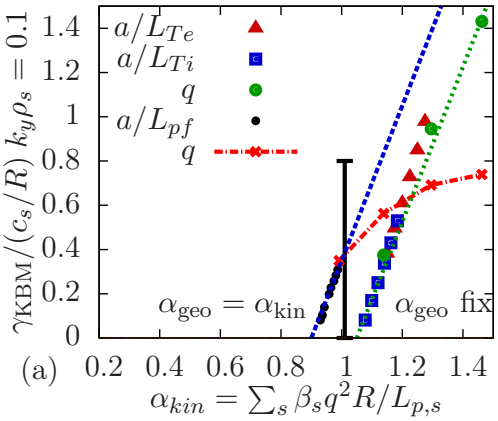

Figure 4: (a)KBM/BAE growth rate, scanning various components of α_{kin}, such as q and gradients based on the q=1.54 eq. case. Keeping consistent $\alpha_{\text{geo}} = \alpha_{\text{kin}}$ yields lower threshold. The nominal value is indicated as a vertical line.

V. LINEAR ITG AND KBM PHYSICS INCLUDING FAST IONS

In the following, the impact of fast ions on linear physics is investigated in detail. Increased α_{geo} leads to geometric stabilization of modes, especially the KBM/BAE, as reported also in Ref. [41], for example. On the other hand, fast ions dilute the main plasma, which reduces ITG drive, but they can also dynamically contribute to the plasma fluctuations and excite fast-particle modes, such that KBM/BAE drive is enhanced. The dynamic impact on ITG can be stabilising or de-stabilising, depending mainly on the fast ion gradient.

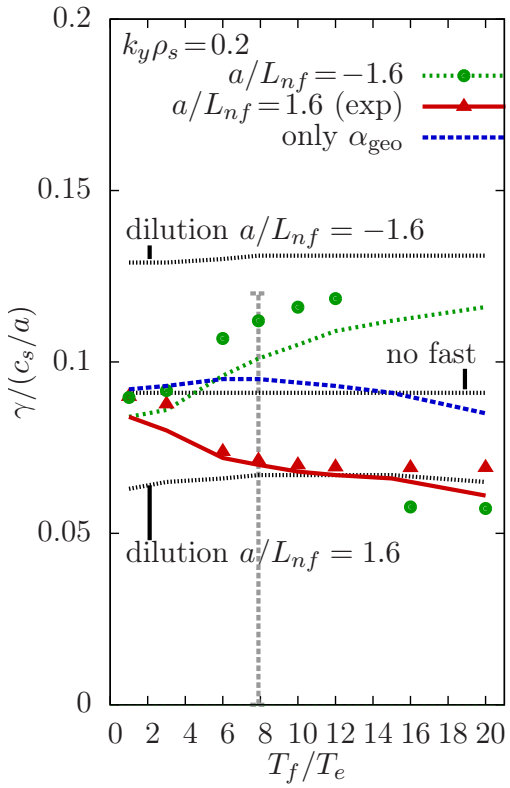

Figure 5: Temperature dependence of fast ion stabilisation: Increasing T_f reduces the active role of fast ions. The dilution limit (no active beam ions, n_D, a/L_{nD} and $\alpha_{\rm geo}$ as in full physics) is approached at high T_f. Negative a/L_{nf} reverses the direction of fast ion effects (see text). The geometric stabilisation is weak for ITG, as seen in scanning only $\alpha_{\rm geo}$ with $n_D = n_e$, $a/L_{nD} = a/L_{ne}$. Results without fast ions and $\alpha_{\rm geo}$ from thermal pressure are labelled as "no fast". Symbols are TGLF for the full physics case. The experimental T_f is indicated as a vertical line.

KBM physics is characterised by a critical threshold in $\alpha_{\rm kin}$. Unlike ITG, the nonlinear KBM threshold largely coincides with the linear one [5]. Figure 4(a) shows that KBM/BAE modes become unstable when $\alpha_{\rm kin} > 0.8$, be it due to thermal or fast particle gradients, or q. Here, the geometric $\alpha_{\rm geo}$ is kept consistent with $\alpha_{\rm kin}$. For $q = 1.54$, KBM stability is reached at 20% reduced fast ion gradient, if the geometric $\alpha_{\rm geo}$ is fixed to the nominal value. As $\alpha \propto q^2$, KBM physics is strongly sensitive to the q profile: Indeed, the q=1.34 equilibrium is KBM/BAE stable with nominal parameters, but still close to threshold. The infinite-n ballooning limit of magneto-hydrodynamics (MHD) is often used as a proxi for KBM stability. In a circular cross-section, the limit $\alpha_{\rm crit,mhd} \sim 0.6s$ is found for $s \gtrsim 0.5$, which would correspond to $\alpha_{\rm crit} = 0.46$ to 0.26 for $\hat{s} = 0.77$ and 0.44, respectively. Presumably due to plasma shaping, we have much larger $\alpha_{\rm crit} \sim 0.8$ in ASDEX Upgrade non-inductive plasmas. For $\rho_{\rm tor} = 0.4$ we confirmed that increasing local triangularity and/or elongation yields an even larger KBM/BAE threshold.

Radial profile variations in temperature, density and geometry are not included in this work. However, in low magnetic shear JET core plasmas [41], as well as JET pedestal cases, [42], such global effects significantly increase the KBM threshold. This trend is confirmed in a circular plasma at $k_y\rho_s \approx 0.3$ [43]. Also for the present ASDEX Upgrade scenario, preliminary results indicate a KBM/BAE threshold up-shift due to global effects, especially in regions $\rho_{\rm tor} < 0.4$.

For NSTX edge plasmas, access to the second stability regime was documented, where increased α suppresses KBM when geometry and gradients are consistently linked [44]. The core of AUG non-inductive plasmas is clearly not in the second stability regime, though.

Besides lowering the ballooning threshold, fast ions can actively take part in thermal ITG dynamics [12], provided they are not too energetic. In the full dilution limit $T_f/T_e \gg 1$, drift velocity and gyro-orbits are large, so that fast ion effects are restricted to reducing the main ion density and gradient [9]. However, the intermediate temperatures reached by external heating in present-day devices still allow a dynamic contribution, which can be stabilising or de-stabilising, mainly depending on the sign of ∇F_{0f}. As further detailed in Ref. [27], this interaction is mainly through a contribution to the electrostatic potential fluctuations. Since fast ions barely carry fluctuating current, any interplay with magnetic fluctuations is indirect. ASDEX Upgrade non-inductive plasmas feature a dominant (positive) a/L_{nf} from NBI heating, in which case fast ions are always de-stabilising as compared to the dilution limit, but they are less effective than thermal ions. This is demonstrated in Fig. 5 for the $k_y\rho_s = 0.2$ ITG mode. For the nominal temperature $T_f = 7.8T_e \sim 25keV$, dilution is almost complete. Negative a/L_{nf} leads to increased thermal a/L_{nD} (through quasi-neutrality) so that increased ITG growthrates are found, even though the active contribution of fast ions is stabilising. Geometric stabilisation is small compared to the dynamic contributions, as confirmed in a two-species setup, without fast ions, only varying the geometric factor $\alpha_{\rm geo}$ consistent with T_f. As a side note, all fast ion effects are cancelled, when ∇F_{0f} is set. Hollow or flat fast ion profiles could be experimentally realised in cases of strongly off-axis external heating, but are not expected for fusion born alpha particles in a reactor plasma.

Concluding this section, the previously assumed hypothesis of fast ions dynamically stabilising ITG by adding to $\alpha = \alpha_{\rm th} + \alpha_{\rm fast}$ through nonlinear EM stabilisation can be formulated more precisely:

Externally heated ions in present-day devices are in temperature regimes, in which increased T_f (or ∇T_{0f}) yields more effective stabilisation, and this coincides with increased α. This trend is not universal, though: For beam ions, a/L_{nf} usually dominates ∇F_0, in which case complete dilution towards $T_f \gg T_e$ yields maximum stabilisation. Additionally, large a/L_{nf} can enforce flat a/L_{nD} through quasi-neutrality, which can reduce ITG as well. Active fast-ion stabilisation beyond dilution can be achieved when a/L_{Tf} is much larger than a/L_{nf}, which is typical for ICRH heated plasmas. As detailed in Ref. [27], this process is enhanced by a resonance of ITG modes with the fast-ion magnetic drift $\omega_{Df} = T_f/Z_f\omega_{Di}$, and therefore allows optimisation of fast ion parameters in intermediate temperature regimes. Highly energetic fusion born alpha particles with $T_f \sim 80T_e$ are well described in the full dilution limit. This is because they can not resonate with ITG and gyro-averaging is effective in removing their contribution to ϕ. For optimising fast ion stabilisation under reactor conditions, introducing additional ICRH heating of thermal ions or minorities remains an option, unless the KBM/BEA limit is surpassed. The linear physics discussed in this section is found to carry over to the nonlinear regime, whereby the reduction of turbulence levels can be stronger than the reduction of growth rates. For making quantitative predictions, the details of the interplay with nonlinear electromagnetic effects, as well as the impact of fast ions on zonal flows are still under investigation.

VI. COMPARISON TO QUASILINEAR TRANSPORT MODELLING

Obtaining the results presented in the previous sections requires a significant investment of time and computing resources. While helping to identify key physics ingredients for understanding advanced scenarios, simplified tools are needed for exploring a great variety of scenario designs. Developments must build on insights gained from nonlinear gyrokinetic simulations. Here, we compare GENE results to the trapped Gyro-Landau-Fluid code TGLF with the ultimate goal of extending its applicability regime to the present scenario. The employed TGLF version [45] includes an improvement, which allows the correct treatment of shaping effects in Ampére's law by considering a corresponding factor of $(B_{\rm unit}/B_0)^2$. In the present ASDEX Upgrade case, $B_{\rm unit} = q/r\,\mathrm{d}\psi/\mathrm{d}r = 1.36B_0$ with ψ the poloidal flux divided by 2π, and B_0 is the field on the magnetic axis. The same time-averaged parameters ($q = 1.34$) are used for both codes and

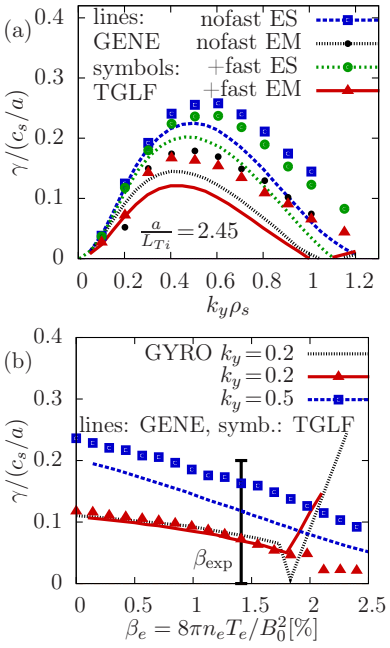

Figure 6: Comparison of linear GENE (lines) to TGLF simulations (symbols) in the q=1.34 case: (a) growth rate (k_y) (b) β stabilisation for $k_y = 0.2, 0.5$. The pressure gradient is consistent with the kinetic profiles in all runs ($\alpha_{\rm geo} = \alpha_{\rm kin}$) and include fast ions.

converted, where necessary. Notable TGLF numeric settings are `nbasis_max=8`, `width_max=2`, `filter=2.6`, `use_mhd_rule=T`. The geometric pressure $\alpha_{\rm geo}$(GENE) and `p_prime`(TGLF) are consistent with $\alpha_{\rm kin}$ in all linear scans in this section. This means $\alpha_{\rm geo} = 0$ in ES cases, deviating from the setup in the previous sections. The complete TGLF input file can be found in the online supplementary material for this paper. Figure 6 shows that for low wavenumbers GENE and TGLF largely agree in the linear ITG physics in the cases with or without fast particles or EM effects. A benchmark between GENE and GYRO [46] shows agreement in the ITG-KBM/BAE transition between both codes. For $k_y > 0.3$ GENE computes lower growth rates than TGLF, but linear β stabilisation is similar in both codes. At $k_y\rho_s = 0.2$, even the T_f dependence is captured in Fig. 5. For the EM simulations, the TGLF filter parameter is required to suppress Alfvénic modes appearing at β values below the experimental value at $k_y\rho_s = 0.2$, suggesting that improvements are necessary for TGLF to describe KBM/BAE physics. The correct treatment of pressure gradient terms, as well as $B_\parallel$ is important for the present highly electromagnetic case. Switching off $B_\parallel$ in GENE simulations, the KBM threshold is correct only when also the pressure-gradient term $-v_\perp^2\, 2\pi\nabla p/B_0^2$ is subtracted from the ∇B-drift, as in Ref. [37]. Since ac-

curate description of $B_\parallel$ fluctuations in fluid models is severely constrained by closure conditions, it is thus recommended to compensate them by subtracting this ∇p term. In TGLF this is achieved by using the MHD rule.

Comparing GENE nonlinear and TGLF quasilinear results in Fig. 7(a), it is obvious that nonlinear EM stabilisation is not sufficiently strong in TGLF. It is well known that highly electromagnetic turbulence can feature a strong up-shift of its a/L_{Ti} threshold with respect to linear physics. While the precise physics mechanism and its implications for quasilinear modelling is still under investigation, a correlation with relatively stronger zonal flow action is already identified [6, 8]. It may thus be interesting to extend saturation rules similar to TGLF SAT1 [18], by adapting the zonal flow strength with β.

Comparing turbulent and quasilinear spectra in Fig. 7(b), we observe that the strong overprediction of transport in TGLF origins mainly from $0.2 < k_y < 0.7$, the region where also the growth rates are somewhat larger in TGLF as compared to GENE. The spectral fall-off for $k_y > 0.7$ coincides, and the spectral peak of Q_i is found at about $k_y = 0.3$ in all cases. It is recommended to increase the k_y mode density in TGLF, though. The main extensions necessary for TGLF to describe the present parameter regime are (i) slightly reduced ITG growth rates for $k_y > 0.3$ (ii) avoid too early KBM transition (iii) extend the saturation rule to strongly EM cases. For the saturation rule, beta-scaling of zonal flow action may be explored.

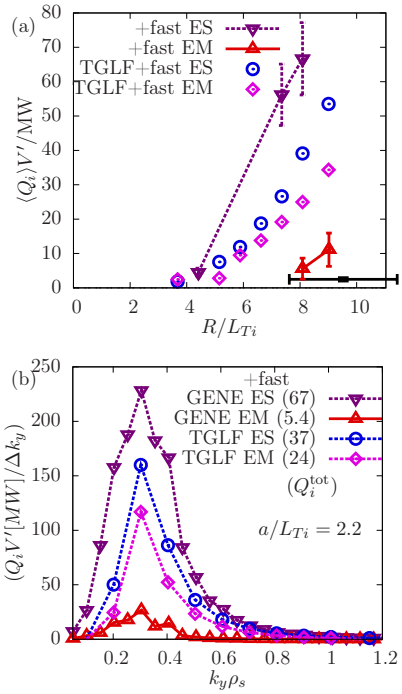

Figure 7: Comparison of nonlinear GENE to quasilinear TGLF quasilinear q=1.34: (a) Ion flux-gradient relation (ES uses $\alpha_{\rm tot}$ and according `p_prime` (b) Ion energy flux spectra for $a/L_{Ti} = 2.2$, total $Q_i V'/MW$ in brackets.

VII. CONCLUSIONS

Concluding on our results, the present AUG discharge features an enhanced T_i peaking due accessing a strongly stabilised ITG regime. Nonlinear Gyrokinetic simulations can reconcile the experimental fluxes, when nonlinear electromagnetic effects, as well as dynamic fast ions and their pressure contribution to the equilibrium are included. Importantly, geometric stabilisation is not sufficient to fully suppress ion-scale turbulence. Modelling this regime with TGLF requires improvements in capturing the KBM limit, as well as nonlinear electromagnetic physics.

A q-profile sensitivity study showed that the KBM/BAE threshold very close to the experimental operation point. High transport levels of particles and heat for all species are found in the KBM/BAE regime, from which we deduce that this turbulence type must be stable or marginally stable. This situation is very similar to the analysis of several other plasmas with particularly good confinement properties, reaching from L-mode [12] to H-mode plasmas of the hybrid type at JET [8, 13, 14] and ^{3}He minority ICRH heated H-modes at ASDEX Upgrade [47, 48].

The analysis of these cases indicates that optimal ITG stabilisation, and thus improved confinement is obtained by closely approaching the KBM/BAE limit from below (not surpassing it). This could, for example, be achieved by tailoring the q profile.

On the other hand, the overall plasma stability is related to the MHD ideal no-wall limit which poses constraints on the q profile as well, especially when β_N is desired to be large [49]. Indeed, both global MHD stability and KBM/BAE stability are linked through a threshold in the normalised pressure $\alpha_{\rm kin}$. Even though it is known that profile effects further increase the KBM β-limit, the closeness to the KBM/BAE threshold is unlikely to be pure coincidence. Thus, the question arises, whether small-scale KBM/BAE turbulent transport can ultimately regulate the fast and thermal pressure profiles, before large-scale MHD modes can destroy the improved confinement or even disrupt the plasma.

Apparently, the present ASDEX Upgrade β_N controlled non-inductive discharges, as well as the above mentioned JET hybrids are still stable to

disruptive modes. However, similar discharges have been performed at ASDEX Upgrade, in which further increase of β_N brings the plasma sufficiently close to the no-wall limit to destabilise large-scale MHD modes, resulting in drastic reduction of the confinement quality [50]. Precursor modes have been identified in the magnetic fluctuation measurements, which could be of BAE type and may have triggered the $n = 1$ mode.

Following the experience from electromagnetic simulations that $E \times B$ flow shear is of limited relevance, and that that the critical a/L_{Ti} increases with increasing q, it may be feasible to experimentally determine the turbulence regime of non-inductive plasmas. We propose to raise the central q profile—in otherwise equivalent conditions—and observe the result: Increased core confinement (or rather pressure gradient) would indicate that the ITG regime gets further stabilised towards the optimal state. Lower pressure peaking in a stable discharge would indicate that KBM/BAE turbulence already limits the profiles. Finally, the appearance of large scale modes or disruptions would indicate that MHD modes restrict the operation regime. In the latter case, transport could still be ITG limited, offering possibilities of further optimisation. Stable scenarios with further reduced ion transport can then only exist when MHD modes are actively mitigated [51]. At ASDEX Upgrade, experiments in this direction are possible using counter-ECCD in the plasma center.

It has to be kept in mind that in the outer core positions $\rho_{\text{tor}} \sim 0.5 - 0.8$ turbulence is typically of more electrostatic character. Here, elevating q is expected to de-crease ITG thresholds and reduce flow shear efficiency. Besides edge physics, the interplay of more electromagnetic turbulent transport in the inner core and more electrostatic turbulence in the outer core will determine the global confinement quality.

Insights from such experiments, as well as more detailed nonlinear gyrokinetic parameter scans (involving further radial positions, or even radially global simulations), can be applied to the development of q-profile optimised scenarios for ITER and DEMO. Quasilinear modelling capabilities require improvements on capturing the KBM limit more accurately, as well as extending the nonlinear saturation rule for ITG to the strongly electromagnetic regime.

Acknowledgements

The authors would like to thank C. Angioni, E. Poli, M. J. Pueschel and D. Told for valuable discussions, as well as G. Staebler for providing TGLF support.

This work has been carried out within the framework of the EUROfusion Consortium and has received funding from the Euratom research and training programme 2014-2018 under grant agreement No 633053. The views and opinions expressed herein do not necessarily reflect those of the European Commission.

The numerical results presented in this work were carried out using the HELIOS supercomputer system at the Computational Simulation Centre of International Fusion Energy Research Centre (IFERC-CSC), Aomori, Japan, under the Broader Approach collaboration between Euratom and Japan, implemented by Fusion for Energy and JAEA, the resources of the MPCDF computing center, Garching, Germany, and the MARCONI supercomputer system at CINECA, Italy.

References

[1] A. Bock, in *EPS Meeting Abstracts O3.110* (2016).
[2] J. Stober, in *"Advanced tokamak experiments in full-W ASDEX Upgrade"*, Preprint: 2016 IAEA Fusion Energy Conference, Kyoto, post-deadline (2016).
[3] A. Bock, et al., Nucl. Fusion (2017). *doi:10.1088/1741-4326/aa8967*
[4] J. Candy, Phys. Plasmas **12**, 072307 (2005).
[5] M. J. Pueschel, M. Kammerer, and F. Jenko, Phys. Plasmas **15**, 102310 (2008).
[6] M. J. Pueschel and F. Jenko, Phys. Plasmas **17**, 062307 (2010).
[7] M. J. Pueschel, T. Görler, F. Jenko, D. R. Hatch, and A. J. Cianciara, Phys. Plasmas **20**, 102308 (2013).
[8] J. Citrin, et al., Plasma Phys. Control. Fusion **57**, 014032 (2015).
[9] G. Tardini, et al., Nucl. Fusion **47**, 280 (2007).
[10] C. Angioni and A. G. Peeters, Phys. Plasmas **15**, 052307 (2008).
[11] C. Holland, C. C. Petty, L. Schmitz, K. H. Burrell, G. R. McKee, T. L. Rhodes, and J. Candy, Nucl. Fusion **52**, 114007 (2012).
[12] J. Citrin, F. Jenko, P. Mantica, D. Told, C. Bourdelle, J. Garcia, J. W. Haverkort, G. M. D. Hogeweij, T. Johnson, and M. J. Pueschel, Phys. Rev. Lett. **111**, 155001 (2013).
[13] J. Garcia, C. Challis, J. Citrin, H. Doerk, G. Giruzzi, T. Görler, F. Jenko, P. Maget, and JET Contributors, Nucl. Fusion **55**, 053007 (2015).
[14] H. Doerk, C. Challis, J. Citrin, J. Garcia, T. Gör-

ler, F. Jenko, and J. Contributors, Plasma Phys. Control. Fusion **58**, 115005 (2016).
[15] G. J. Wilkie, I. Pusztai, I. Abel, W. Dorland, and T. Fülöp, Plasma Phys. Control. Fusion **59**, 044007 (2017).
[16] G. M. Staebler, J. E. Kinsey, and R. E. Waltz, Phys. Plasmas **12**, 102508 (2005).
[17] G. M. Staebler, J. E. Kinsey, and R. E. Waltz, Phys. Plasmas **14**, 055909 (2007).
[18] G. M. Staebler, N. T. Howard, J. Candy, and C. Holland, Nucl. Fusion **57**, 066046 (2017).
[19] P. Mantica, in *APS Meeting Abstracts* (2016).
[20] P. Mantica, et al., Nucl. Fusion **57**, 087001 (2017).
[21] A. Bock, Dissertation, Ludwig-Maximilians-Universität München (2016).
[22] H. Zohm, A. Bock, E. Fable, J. Stober, and F. Traeuble, in *APS Meeting Abstracts* (2016).
[23] G. V. Pereverzev and P. N. Yushamanov, ASTRA automated system for transport analysis in a tokamak Technical Report IPP, Garching, Germany **5/98** (2002).
[24] E. Fable, C. Angioni, A. A. Ivanov, K. Lackner, O. Maj, S. Y. Medvedev, G. Pautasso, G. V. Pereverzev, W. Treutterer, and the ASDEX Upgrade Team, Plasma Phys. Control. Fusion **55**, 074007 (2013).
[25] C. C. Petty, et al., Nucl. Fusion **56**, 016016 (2016).
[26] F. Sommer, et al., Nucl. Fusion **55**, 033006 (2015).
[27] A. Di Siena, T. Görler, H. Doerk, and E. Poli, Fast-ion stabilization of tokamak plasma turbulence, submitted to Phys. Rev. Lett.
[28] A. Pankin, D. McCune, R. Andre, G. Bateman, and A. Kritz, Comput. Phys. Commun. **159**, 157 (2004).
[29] *TRANSP home page, http://w3.pppl.gov/transp.*
[30] R. Fischer, et al., Fusion Science and Technology **69** (2016).
[31] R. Fischer, in *EPS Meeting Abstracts P1.016* (2016).
[32] F. Jenko, W. Dorland, M. Kotschenreuther, and B. N. Rogers, Phys. Plasmas **7**, 1904 (2000).
[33] www.genecode.org, *development version GIT#dbedae7e* (2017).
[34] A. Di Siena, T. Görler, H. Doerk, J. Citrin, T. Johnson, M. Schneider, E. Poli, and JET Contributors, J. Phys.: Conf. Ser. **775** (2016).
[35] C. Bourdelle, G. T. Hoang, X. Litaudon, C. M. Roach, T. Tala, ITPA Topical Group on Transport, I. Physics, and International ITB Database Working Group, Nucl. Fusion **45**, 110 (2005).
[36] M. Romanelli, A. Zocco, F. Crisanti, and JET EFDA Contributors, Plasma Phys. Control. Fusion **52**, 045007 (2010).
[37] N. Joiner, A. Hirose, and W. Dorland, Phys. Plasmas **17**, 072104 (2010).
[38] J. E. Kinsey, R. E. Waltz, and J. Candy, Phys. Plasmas **12**, 062302 (2005).
[39] F. Jenko, W. Dorland, and G. W. Hammett, Phys. Plasmas **8**, 4096 (2001).
[40] J. Citrin, F. Jenko, P. Mantica, D. Told, C. Bourdelle, R. Dumont, J. Garcia, J. W. Haverkort, G. M. D. Hogeweij, T. Johnson, et al., Nucl. Fusion **54**, 023008 (2014).
[41] S. Moradi, I. Pusztai, I. Voitsekhovitch, L. Garzotti, C. Bourdelle, M. J. Pueschel, I. Lupelli, M. Romanelli, and t. JET-EFDA Contributors, Nucl. Fusion **54**, 123016 (2014), 1411.4904.
[42] D. R. Hatch, M. Kotschenreuther, S. Mahajan, P. Valanju, F. Jenko, D. Told, T. Görler, and S. Saarelma, Nucl. Fusion **56**, 104003 (2016).
[43] T. Görler, N. Tronko, W. A. Hornsby, A. Bottino, R. Kleiber, C. Norscini, V. Grandgirard, F. Jenko, and E. Sonnendrücker, Phys. Plasmas **23**, 072503 (2016).
[44] J. Canik, W. Guttenfelder, R. Maingi, T. Osborne, S. Kubota, Y. Ren, R. Bell, H. Kugel, B. LeBlanc, and V. Souhkanovskii, Nucl. Fusion **53**, 113016 (2013).
[45] *TGLF download from github, 25th Apr. 2017.*
[46] J. Candy and R. Waltz, J. Comput. Phys. **186**, 545 (2003), ISSN 0021-9991.
[47] M. J. Mantsinen, R. Bilato, V. V. Bobkov, A. Kappatou, R. M. McDermott, M. Nocente, T. Odstrčil, G. Tardini, M. Bernert, R. Dux, et al., AIP Proceedings **1689** (2015).
[48] F. N. de Oliveira, et al., in *EPS Meeting Abstracts P2.176* (2017).
[49] V. Igochine, et al., Nucl. Fusion **57**, 116027 (2017).
[50] P. Piovesan, et al., Plasma Phys. Control. Fusion **59**, 014027 (2017).
[51] M. Reich, Real-time control of NTMs using ECCD at ASDEX Upgrade PPC/P1-26, *paper presented at 25th IAEA Int. Conf. on Fusion Energy St Petersburg* 2014.